ADVANCED ELECTROMAGNETICS, Vol. 3, No. 1, April 2014

Reconsidering Ampere's Double Layer Representation for Magnetic Field Evaluation in a NDE Detection of a Zero Volume Crack

Michel Poloujadoff, Laroussi Bettaieb, and Hamid Kokabi

Université Pierre et Marie Curie (UPMC), Laboratoire d'Électronique et Électromagnétisme (L2E),
Aile 65/66 – 2ème étage - 4, Place Jussieu 75252 Paris Cedex 05.
laroussi.bettaieb@gmail.com; hamid.kokabi@upmc.fr; michel.poloujadoff@upmc.fr

Abstract

The paper has two different objectives. The first one is to show that Ampere's double layer method, which is equivalent to one of the Maxwell equations, leads to the integration of a simple closed form expression, thus avoiding the need to solve complicated partial differential equations. The second aim is to study the case of a zero volume defect in a NDE problem by a perturbation method and the introduction of a double layer. The combination of these two techniques leads to a very fast solution of the problem. A practical example including an experimental check is given.

Keywords: Ampere's double layer, eddy currents, fictitious sources, magnetic field evaluation, NDE, perturbation method, zero volume crack.

1. Introduction

The purpose of this paper is two-fold. Initially, we wanted to study the NDE detection of a zero volume crack in an aluminum plate. For us, on the hand, this problem was a practical, industrial problem. And on the other hand, it was a didactical electromagnetic problem.

Indeed, the so called Maxwell equations are four partial differential equations which are the basis of most studies of electromagnetic systems. This is true for Non Destructive Evaluation methods [1 to 22]. The reason is that this model is considered as the "most beautiful" representation of electromagnetic phenomena or, at least the most general. The consequence is that most modern textbooks devoted to electromagnetic have banished the original expressions established by Ampere himself, which are closed from expressions.

2. Presentation of an example

Non Destructive Evaluation (NDE) can be considered as a method which allows to detect a flaw (here: a crack) in a metallic conducting plate, without modifying it.

More specifically, if we create an alternating magnetic field in a metallic object, this leads to the creation of eddy currents, which in turn create a magnetic reaction field. Conducting this experiment first with a flawless reference object, then with another object, seemingly identical to the first one, differences between the reaction fields may reveal internal differences, essentially flaws.

In the present paper, we consider a flawless aluminum plate whose dimensions are $(100\,mm \times 110\,mm \times 5\,mm)$, and resistivity $\rho = 5.82 * 10^{-8} \Omega.m$ (AG3 alloy at 20°C). We create a uniform alternating field $\vec{B}_{exc} = B_m \cos(\omega t)\overrightarrow{Ox}$ (amplitude $B_m = 6.74 * 10^{-4} T$, frequency $f = 180 Hz$) (see figure 1 (a)), and we evaluate the field of the eddy currents. The skin depth of aluminum at 180Hz (9.11mm) is twice as large as the plate thickness (5mm).

The question to be answered is: what would be the difference if we consider another plate of same dimensions and resistivity, but with a null volume crack as shown in figure 1 (b)?

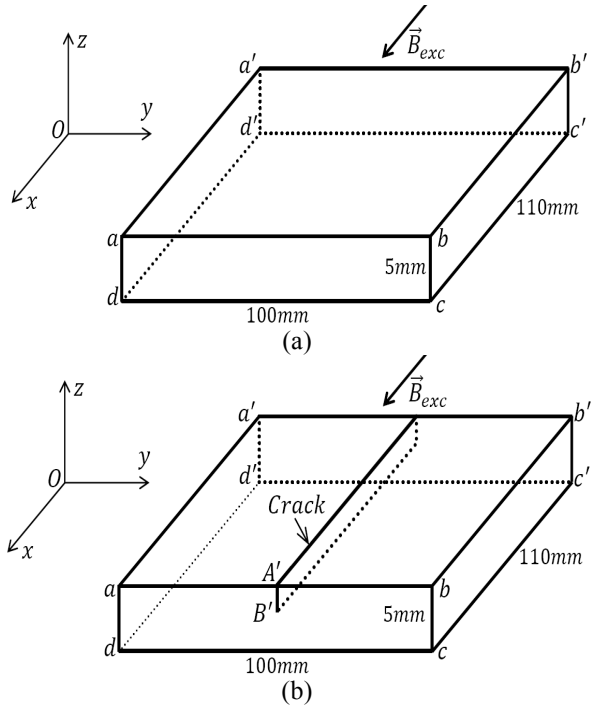

Figure 1: Description of a flawless plate (a) and a defective one (b)

3. Method of analysis

3.1. Flawless plate

The first step is to analyze the case of the flawless plate, and this is rather simple. Indeed, in the present case, the standard penetration depth in the plate at $180Hz$ is $9.11mm$, which means that skin effect is negligible, so the induced currents are just proportional to the time derivative of the vector potential of the exciting field (see appendix 1). The current density in the flawless plate is shown in figures 2 (a) and 2 (b).

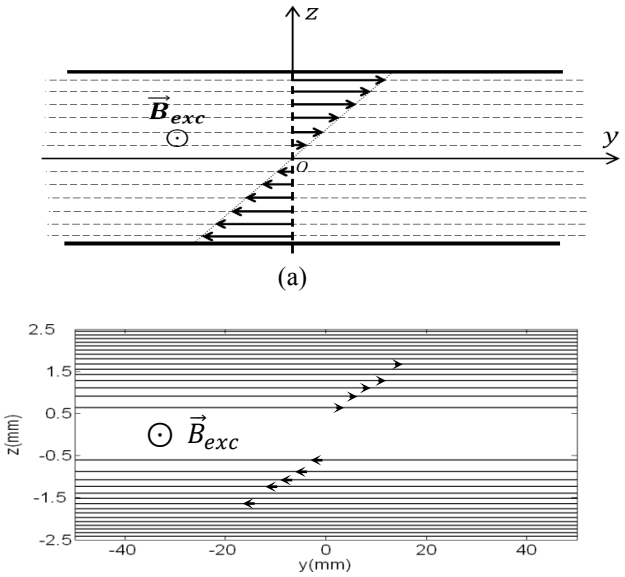

Figure 2: Description of the eddy currents densities (a) and lines (b) in the abcd plane, in the case of a flawless plate. (with B_{exc})

Note that the induced current is parallel to Oy axis principally except at the extremities of the plate which are not shown on the figure 2 (b).

The figures 2 (a) and 2 (b) represent the same situation in which the flawless plate is located in an external excitation field. The figure 2 (a) shows the schematic variation of the eddy current density (decreasing with z) and the figure 2 (b) illustrates the calculated eddy current lines for a flawless plate considered very large in y direction.

As it is defined in the above figures, we consider an excitation induction field B_{exc} parallel to Ox axis (see figure 1), and we study the currents produced in the planes which are parallel to plane $abcd$, and therefore normal to Ox. The currents densities described in figure 2 (a) are governed by the fundamental Maxwell's equations:

$$\partial j_y/\partial y + \partial j_z/\partial z = 0 \ (\vec{\nabla}.\vec{j} = 0) \tag{1}$$

In fact, The Maxwell Ampere equation is given by:

$$\vec{\nabla}\Lambda\vec{B} = \mu_0\vec{j} + \mu_0\varepsilon_0\frac{\partial\vec{E}}{\partial t}, \tag{2}$$

and we have also:

$$\vec{\nabla}.\vec{B} = 0, \text{ and } \vec{\nabla}\Lambda\vec{E} = -\frac{\partial\vec{B}}{\partial t}. \tag{3}$$

Besides:

$$\vec{\nabla}\Lambda(\vec{\nabla}\Lambda\overrightarrow{B}) = grad(\vec{\nabla}.\vec{B}) - \Delta\vec{B}. \tag{4}$$

These equations allow reaching the following expression:

$$\mu_0\vec{\nabla}\Lambda\vec{j} = -\Delta\vec{B} + \mu_0\varepsilon_0\frac{\partial\vec{B}^2}{dt^2} \text{ (with } \mu_0\varepsilon_0 = \frac{1}{C^2}) \tag{5}$$

Therefore, the equation (5) is deduced from the equations 2, 3 and 4 with the presence of an external excitation field and it is related to the figures 2 (a) and 2 (b).

In our case, the magnetic excitation is along $\overrightarrow{Ox}$ direction and the sample is located in the uniform part of the excitation magnetic field. For a flawless plate, the eddy currents are unperturbed as shown on figure 2. The magnetic field created by the eddy currents along x axis and opposite to excitation field (B_{exc}) is very small comparing to the B_{exc}.

Besides, as the frequency of this excitation magnetic field is very low (180Hz) and as $\frac{1}{C^2}$ is very small, so the term $\mu_0\varepsilon_0\frac{\partial\vec{B}^2}{dt^2}$ is approximately zero.

3.2. First approach to the analysis of a defective plate: Introduction of a perturbation method

The second step is to determine the currents in the defective plate. Two possibilities exist. Indeed, we may either directly evaluate the currents, or directly evaluate the difference between the currents in the flawless and in the defective plates. In both cases, we shall have the choice between using a double Fourier series expansion or a finite element (or finite difference) method. We have chosen to evaluate directly the perturbation introduced by the crack in the induced currents. And we shall see that any finite difference or finite element method leads directly to the characterization of Ampere's layer and to an evaluation of the crack effect.

3.3. Introduction of a numerical determination of the perturbation currents

The existence of the zero volume crack defect between A' and B' as shown in figure 1 (b) is considered equivalent to a fictitious source of currents (see figure 3) whose current densities values are opposite to the values of the current densities existing at the same place in the flawless plate [23 and 24]. This method belongs to the set of so called "perturbation methods", as the well-known methods of Thevenin or Babinet.

In fact in this case the external excitation field is zero (B_{exc}=0) so the equation (5) can lead to $\vec{\nabla}\Lambda\vec{j} = 0$ from which the equation (6) can be deduced.

$$\partial j_y/\partial z - \partial j_z/\partial y = 0 \tag{6}$$

The equation (6) is related to the figures 3 and 4 where B_{exc}=0 and the zero volume crack defect is considered as a fictitious source of current.

Equations (1) and (6) are both satisfied if there exists a function Q (called: current function) such that:

$$\begin{cases} j_y = -\partial Q/\partial z \\ j_z = \partial Q/\partial y \end{cases} \quad (7)$$

with:

$$\partial^2 Q/\partial y^2 + \partial^2 Q/\partial z^2 = 0. \quad (8)$$

Note that equation (7) is obtained from (1) and equation (8) from (2).

The boundary conditions are specified in figure 3, with $\partial Q/\partial y = 0$ (symmetry with respect to Oz (i.e. $j_z \equiv 0$)) and also Q is a parabolic function of z between A' and B' for $y = 0$. In fact, this current function Q which is a primitive of the current density (linear function) becomes a parabolic function.

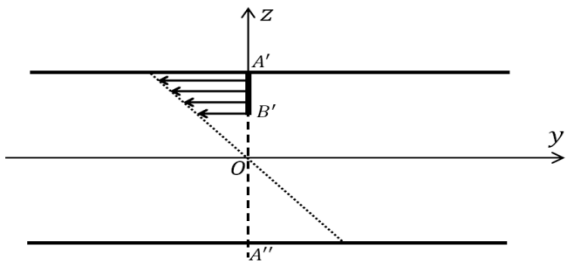

Figure 3: Fictitious source of current equivalent to the zero volume crack between A' and B' (with B_{exc}=0)

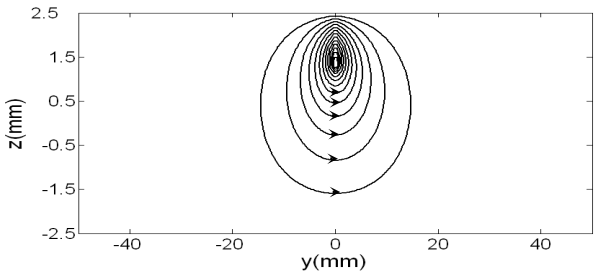

Figure 4: Currents lines generated by the fictitious source representing the zero volume crack between A' and B'

The figures 3 and 4 correspond to the same situation of a plate with a zero volume crack defect with B_{exc}=0. The figure 3 shows the schematic variation of the eddy current density (decreasing with z) and the figure 4 illustrates the calculated eddy current lines for the fictitious source of current representing the defect.

Also $Q \equiv 0$ along the two limits $z = \pm c/2$. These data and conditions suffice to determine the values of $Q(y,z)$ all over the plane by use of any numerical method (series development, finite elements or finite differences methods).

When $Q(y,z)$ is known by any of these well known numerical methods, the lines $Q(y,z) = cte$ are the current lines shown in figure 4. It is clear that Q is dependent absolutely on the crack geometry as it represents the defect as an equivalent fictitious current source.

The combination of the current lines of the unperturbed plate (cf. figure 2 (b)) and of the fictitious source (figure 4) yields the resultant current lines in the defective plate (figure 5) according to the superposition method.

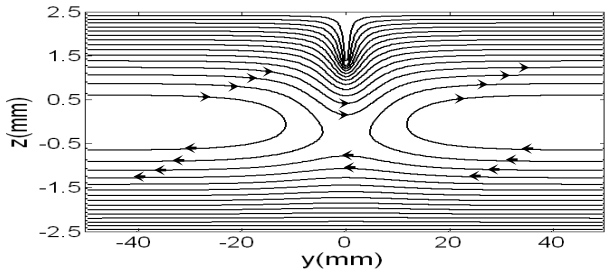

Figure 5: Currents lines in the plate with a perpendicular zero volume crack between A' and B' which represent the additional combination of figures 2 (b) and 4

The induced current is parallel to Oy axis principally except at the extremities of the plate which are not shown on the figure 5. It seems that, from this point, it is easy to evaluate the field created by the induced currents. In fact, this is not so, because of the complicated shape of the current lines. This is why recourse to Ampere's double layer of magnetic masses has been made [25].

3.4. Introduction of Ampere's magnetic masses

The basis of Ampere's magnetic field theory is that a small current loop whose intensity is I, is equivalent to two magnetic masses $\pm dm$, separated by a distance δ, in such a way that $\delta dm = IdS$, I being the loop current, dS the loop surface, δ the distance between the two masses (cf. figure 6 (a)).

It is customary to call $P = \delta.[dm/dS]$ the "power" of the double layer. Therefore the "power" of the double layer is equal to the loop current. The scalar magnetic potential created by a magnetic mass dm at distance r being $dm/4\pi r$, the scalar magnetic potential created by the magnetic dipole (figure 6 (b)), or by the current loop is equal to:

$$V = \delta.[dm/4\pi].[sin\theta/r^2] = [IdS/4\pi].[sin\theta/r^2]. \quad (9)$$

The radial magnetic field is (expressed in A/m):

$$H_r = -\delta.[dm/2\pi].[sin\theta/r^3] = -[IdS/4\pi].[sin\theta/r^3], \quad (10)$$

and the tangential magnetic field it is (expressed in A/m):

$$H_t = \delta.[dm/4\pi].[cos\theta/r^3] = [IdS/4\pi].[cos\theta/r^3]. \quad (11)$$

Therefore, the magnetic field of the eddy currents is extremely easy to evaluate by the repetition of a closed form formula.

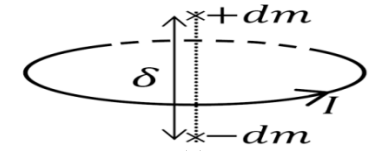

(a)

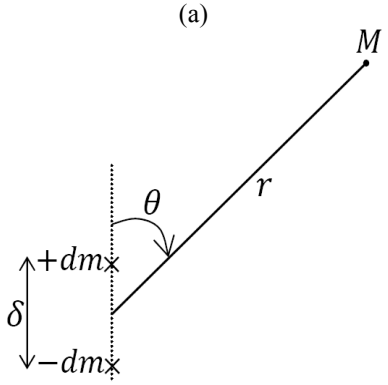

(b)

Figure 6: Definition of Ampere's equivalent magnetic masses

Now, consider a current loop (C), as sketched in figure 7 (a). We do not modify the system by adding additional lines carrying simultaneously two opposite currents $+I$ and $-I$. This system of currents is equivalent to the set of small current loops depicted in figure 7 (b) and 7 (c), with all the currents in the loops being equal to I. Thus, outside the double layer, the magnetic field is the same as the field of the double layer of magnetic masses if its density is equal to $\pm I/\delta$. Ampere has experimentally demonstrated that relationship, which is equivalent to the expression $\vec{I} = rot\vec{H}$, introduced by Maxwell, who called it "Ampere's theorem" as a token of admiration to his predecessor (see appendix 3).

3.5. Relationship between Q and the loop currents densities

In the present case, an important remark is that the function Q, as defined above, happens to be proportional to the loop currents densities y (see figure 8).

$$\int_A^B \vec{j}.\overrightarrow{dl} = \sum_A^B \big((j_1 - j_1 + j_2 - j_2 + j_3 - j_3) + j_4\big).AB = j_4.AB = Q_B - Q_A = Q_B \text{ with } Q_A = 0. \quad (12)$$

3.6. Field created by the fictitious source

We can now come back to figures 1 and 5. Figure 5 shows the lines of currents in any plane parallel to $abcd$ of figure 1(b). Therefore, the current loops in figure 5 represent, in fact, small solenoids parallel to the crack (figure 9 (a)). Each one has to be divided into elementary loops parallel to plane $abcd$. Each loop is equivalent to two layers of opposite signs, so that every layer is cancelled by the next one, except the two extreme ones (see figure 9 (b)).

Therefore, the field of the currents density is equivalent to the field of magnetic masses laying on the two planes $abcd$ and $a'b'c'd'$. At each point, magnetic mass density and Q are equal (expressed in A/m):

$$\frac{dm}{dS} = \frac{I}{L} = Q \text{ (see appendix 3),} \quad (13)$$

where L is the plate length parallel to Ox axis. The field of magnetic masses, being Newtonian, is rather easy to evaluate as explained above.

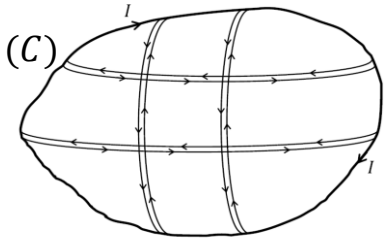

(a)

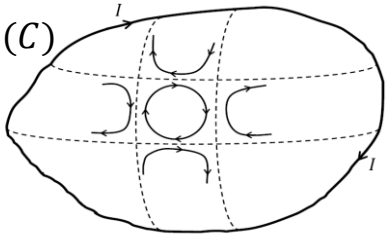

(b)

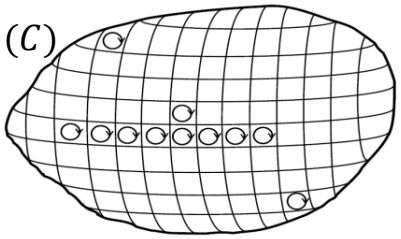

(c)

Figure 7: Set of small current loops equivalent to a large one

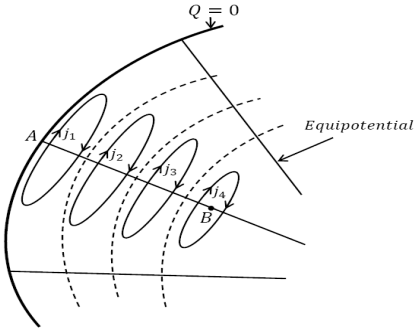

Figure 8: Equivalence of function Q and small loop currents densities

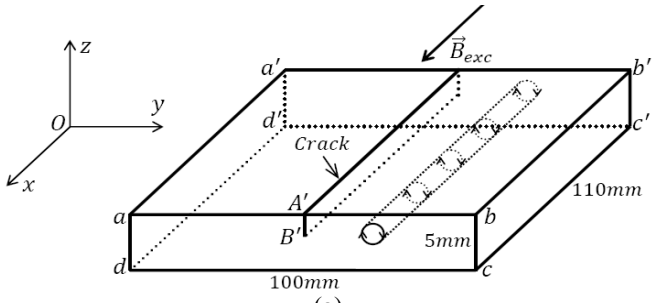

(a)

Figure 9 (a): Small solenoids parallel to the zero volume crack corresponding to the current loops shown in figure 4

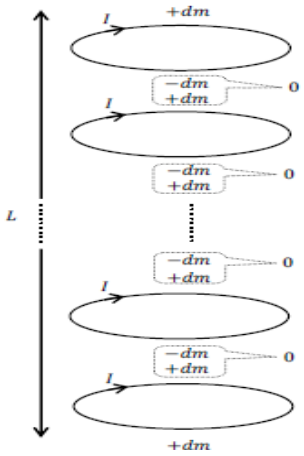

(b)

Figure 9 (b): Reduction of the currents to two layers of magnetic masses at faces $abcd$ and $a'b'c'd'$

3.7. Experimental verification

The theoretical formulation given above has been checked experimentally, with the data given in the introduction. The depth of the crack was $depth = A'B' = 2mm$. The z component of the magnetic field of both the flawless plate and the cracked one are zero at the center of the plate ($x = 0$). For the case $x = 45mm$, the magnetic field is represented by figure 10. The difference of experimental (see appendix 2) and theoretical values is very small (2%), as shown in figure 10.

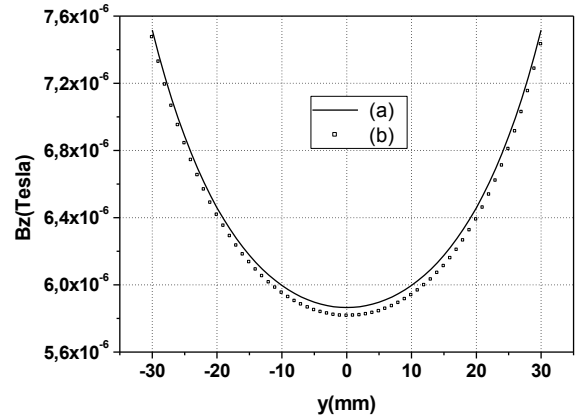

(A)

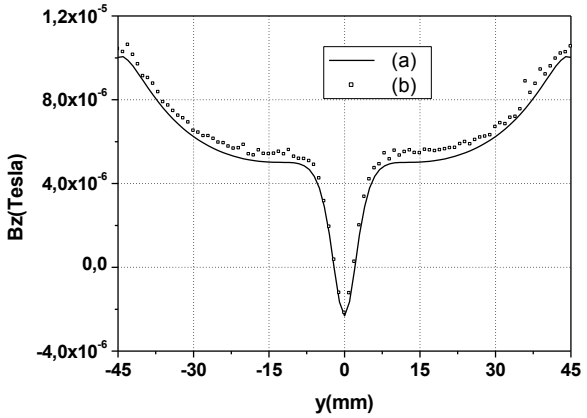

(B)

Figure 10**:** Theoretical (a) and experimental (b) values of B_z in the case of the flawless plate (A), and of the defective (B) one for $x = 45mm$

4. Conclusion

In this paper, we have examined the expression of the magnetic field of induced currents under two different forms. The first is Maxwell's formulation which is a partial differential equation which has to be solved. The second one is Ampere's expression which consists of closed form differential elements which just have to be added up. The latter formulation considerably simplifies the computation process and reduces the computing time.

We have also pointed out that the magnetic masses are easily defined by a current function Q whose spatial derivatives are the current densities.

We have also given an example of a zero volume crack which can be easily represented by an equivalent fictitious source of currents, following the well known Thevenin's or Babinet's principle.

The results have been carefully checked with our experimental set up. Good agreement between theory and experiment has been found.

APPENDIX 1: Induced currents in the flawless plate

For figure 1 (a) and figure 1 (b), we choose a direct reference frame Oxyz with Ox parallel to the induced field and Oz denoting the vertical direction. Thus the potential vector, created by the excitation field inside the plate, at point $M(M_y, M_z)$, is directed in the Oy direction and its value is:

$$A(M_y, M_z) = B * M_z .$$

Since the skin depth of aluminum at $180Hz$ is twice as large as the plate thickness, the corresponding current density is:

$$j_y(M_y, M_z) = \frac{1}{\rho}\frac{\partial A(p_y, p_z)}{\partial t} = \frac{\omega}{\rho} B_m M_z \sin(\omega t),$$

which means that the current lines are parallel to Oy [26 to 30]. As the thickness of the plate (5mm) is very small compared to its length (100mm), the plate can be considered analytically as infinite according to its y-dimension.

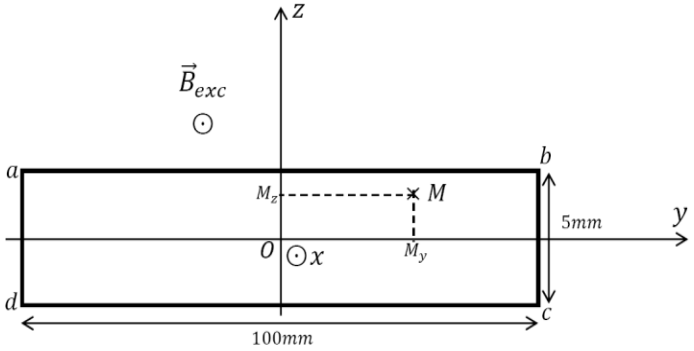

Figure APPENDIX 1: Determination of the induced eddy currents density j_y

APPENDIX 2: Short description of the experimental set up

The excitation field is created by a Helmholtz coil pair H, with a cross section of $12\ mm \times 15\ mm$ each, an external diameter of $240mm$ and with a spacing of $120mm$. The aluminum plate P is mounted on a horizontal stage, thus allowing movement along the x and y directions. The vertical component of the induction field is measured by a sensor S which, in the present case, is a Hall effect micro-sensor [31], associated with a lock-in amplifier which allows a synchronous detection.

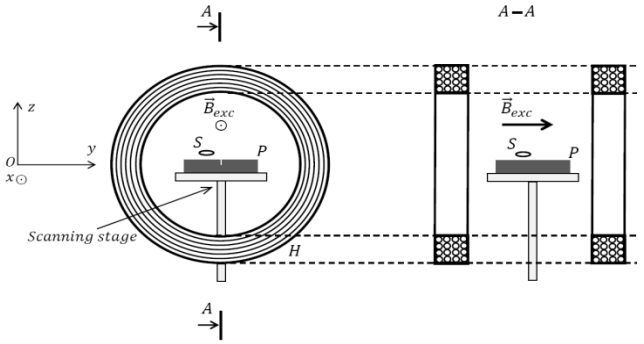

Figure APPENDIX 2: Instrumental set-up

APPENDIX 3: Equivalence between the Ampere's and Maxwell's statements

Consider a current loop I, equivalent to a double layer made of positive and negative charges. The absolute value of the charge density is $\frac{dm}{dS} = \frac{I}{\delta}$. Consider a closed circuit divided in $\widehat{AB}$ and $\widehat{BA}$, where the distance between A and B may become infinitesimally small (figure Appendix 3). According to Poisson's theorem,

$$\oint_{(C)} \vec{H}\vec{dl} = \int_A^B \vec{H}_e\vec{dl} + \int_B^A \vec{H}_i\vec{dl} = 0.$$

Now, $H_i = \frac{dm}{dS}$ is oriented form A to B, and $\int_B^A \vec{H}_i\vec{dl} = -\frac{dm}{dS}\delta$, so that $\int_A^B \vec{H}_e\vec{dl} = -\int_B^A \vec{H}_i\vec{dl} = +\frac{dm}{dS}\delta = I$, which is Maxwell's expression $\oint_{(C)} \vec{H}\vec{dl} = I$, if the distance between A and B is becoming infinitesimally small.

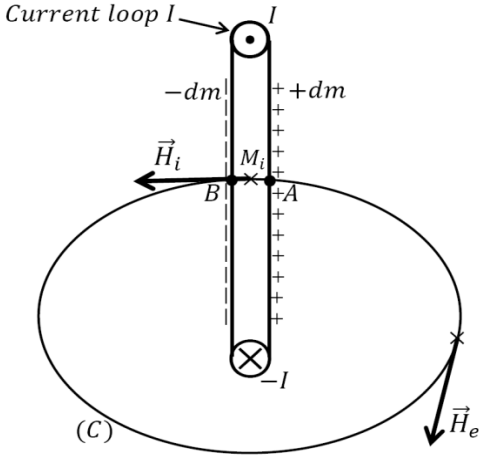

Figure APPENDIX 3: Equivalence between Ampere's and Maxwell's expressions of the Ampere's theorem

Acknowledgment

The authors would like to thank very warmly Dr. Hans-Joachim Krause, researcher and "SQUID applications" Group leader at Forschungszentrum Jülich, for all his advises and the pre reviewing of this paper.

References

[1] Y. Gotoh, A. Kiya, N. Takahashi, Electromagnetic Inspection of Outer Side Defect on Steel Tube With Steel Support Using 3-D Nonlinear FEM Considering Non-Uniform Permeability and Conductivity, IEEE Transaction on Magnetics, vol. 46, no. 8, pp. 3145-3148, 2010.

[2] R. Hamia, C. Cordier, S. Saez, C. Dolabdjian, Eddy-Current Nondestructive Testing Using an Improved GMR Magnetometer and a Single Wire as Inducer: A FEM Performance Analysis, IEEE Trans. Magn., vol. 46, no. 10, pp. 3731–3737, 2010.

[3] C. V. Dodd, W. E. Deeds, Analytical solutions to eddy-current probe-coil problems, Journal of Applied Physics, vol. 39, no. 6, pp. 2829-2838, 1968.

[4] C. V. Dodd, W. E. Deeds, Integral solutions to some eddy current problems, International Journal of Nondestructive Testing, vol. 1, pp. 29-90, 1969.

[5] L. Bettaieb, H. Kokabi, M. Ploujadoff, A. Sentz and A. Tcharkhtchi, Fatigue and/or crack detection in NDE, Nondestructive Testing and Evaluation, vol. 24, no. 4, pp. 1-12, 2009.

[6] Y. Cha, K. H. Kim, J. Shon, Y. H. Kim, and J. Kim, Surface flaws detection using AC magnetic field sensing by a thin film inductive microsensor," IEEE Trans. Magn., vol. 44, no. 11, pp. 4022–4025, 2008.

[7] C. Cordier, S. Saez, S. Lebargy, and C. Dolabdjian, Accurate steel tube axis alignment in nondestructive evaluation probe, IEEE Trans. Magn., vol. 44, no. 10, pp. 2409–2413, 2008.

[8] Y. Hatsukade, S. Okumo, K. Mori, and S. Tanaka, Eddy-current-based SQUID-NDE for detection of surface flaws on copper tubes, IEEE Trans. Appl. Supercond., vol. 17, no. 2, pp. 780–783, 2007.

[9] S. Hirano, Y. Inada, E. Matsumoto, A. Saito, K. Aizawa, M. Matsuda, S. Kuriki, and S. Ohshima, SQUID nondestructive testing system with vibrating normal pick-up coil, IEEE Trans. Appl. Supercond., vol. 17, no. 2, pp. 788–791, 2007.

[10] K. Tsukada, T. Kiwa, T. Kawata, and Y. Ishihara, Low-frequency eddy current imaging using MR sensor detecting tangential magnetic field components for nondestructive evaluation, IEEE Trans. Magn., vol. 42, no. 10, pp. 3315–3317, 2006.

[11] K. Chomsuwan, S. Yamada, M. Iwahara, H. Wakiwaka, and S. Shoji, "Application of eddy current testing technique for high-density doublelayer printed circuit board inspection," IEEE Trans. Magn., vol. 41, no. 10, pp. 3619–3321, 2005.

[12] N. V. Nair, V. R. Melapudi, H. R. Jimenez, X. Liu, Y. Deng, Z. Zeng, L. Udpa, T. J. Moran, and S. S. Udpa, A GMR-based eddy current system for NDE of aircraft structures, IEEE Trans. Magn., vol. 42, no. 10, pp. 3312–3314, 2006.

[13] W. S. Dunbar, The volume integral method of eddy current modeling, Journal of Nondestructive Evaluation, vol. 5, no. 1, pp. 9-14, 1985.

[14] S. M. Nair, J. H. Rose, Electromagnetic induction (eddy currents) in a conducting half-space in the absence of in homogeneities: a new formalism, Journal of Applied Physics, vol. 68, no. 12, pp. 5995-6009, 1990.

[15] Z. Zeng, L. Udpa, S. S. Udpa, and M. S. C. Chan, Reduced magnetic vector potential formulation in the finite element analysis of eddy current nondestructive testing, IEEE Trans. Magn., vol. 45, no. 3, pp. 964–967, 2009.

[16] J. H. McWhirter, J. J. Oravec, and R. W. Haack, Computation of magnetic fields in three-dimensions based on Fredholm integral equations, IEEE Transaction on Magnetics, vol. 18, n° 2, pp. 373-377, 1982.

[17] T. Morisue, A new formulation of the magnetic vector potential method in 3-D multiply connected regions, IEEE Trans. Magn., vol. 24, no. 1, pp. 90–93, 1988.

[18] O. Biro, K. Preis, and W. Renhart, Finite element analysis of 3D multiply connected eddy current problems, IEEE Trans. Magn., vol. 25, no. 5, pp. 4009–4011, 1989.

[19] G. Rubinacci, A. Tamburrino, and S. Ventre, An efficient numerical model for a magnetic core eddy-current probe, IEEE Trans. Magn., vol. 44, no. 6, pp. 1306–1309, 2008.

[20] Y. Le Bihan, J. Pavo and C. Marchand, Calculation of ECT signal of a minute crack by FEMBIM hybrid method, Eur. Phys. J. Appl. Phys., vol. 28, pp. 355-360, 2004.

[21] A. Ruosi, M. Valentino, G. Pepe, V. Monebhurrn, and D. Lesselier, High T_c SQUIDs and eddy-current NDE/: a comprehensive investigation from real data to modeling, Meas. Sci. Techno. vol. 11, pp. 1639-1648, 2000.

[22] J. Bird, T. A. Lipo, A 3-D magnetic charge finite-element model of an electrodynamic wheel, IEEE Transaction on Magnetics, vol. 44, n° 2, pp. 253-265, 2008.

[23] L. Codecasa, P. Dular, R. Specogna, F. Trevisan, A Perturbation Method for the $\mathrm{T}-\Omega$ Geometric Eddy-Current Formulation, IEEE Transaction on Magnetics, vol. 46, no. 8, pp. 3045 - 3048, 2010.

[24] M. Ya. Antimorov, A. A. Kolyshkin, R. Vaillancourt, Application of a perturbation method to the solution of eddy current testing problems, IEEE Transaction on Magnetics, vol. 30, no. 3, pp. 1247-1250, 1994.

[25] I. El Nahas, B. Szabados, M. Poloujadoff, R. Findlay, and X. Wu, A three-dimensional electromagnetic field analysis technique utilizing the magnetic charge concept, IEEE Transaction on Magnetics, vol. 23, no. 5, pp. 3853-3859, 1987.

[26] R. L. Stoll, The analysis of eddy currents, Oxford: Clarendon press, 1974.

[27] L. Bettaieb, H. Kokabi, M. Poloujadoff, A. Sentz, and H. J. Krause, Analysis of Some Non Destructive Evaluation Experiments Using Eddy Currents, Research in Nondestructive Evaluation, vol. 20, no. 3, pp. 159-177, 2009.

[28] L. Bettaieb, H. Kokabi, M. Poloujadoff, A. Sentz, V. Moser, and C. Coillot, Comparison Of The Use Of SQUID an Hall Effect Sensors In NDE, Materials Evaluation, vol. 68, no. 5, pp. 535-541, 2010.

[29] J. A. Tegopoulos and E. E. Kriezis, Eddy currents in linear conducting media, studies in electrical and electronics engineering, vol. 16, Amsterdam: Elsevier, 1985.

[30] C. V. Dodd, The use of computer-modeling for eddy current testing, research techniques in nondestructive testing, vol. III, edited by R. S. Sharpe (ed.). London: Academic Press, pp. 429-479, 1977.

[31] P. Leroy, C. Coillot, V. Mosser, A. Roux and G. Chanteur, Use of magnetic concentrator to highly improve the sensitivity of Hall effect sensors, Sensor Letters, vol. 5, no. 1, pp. 162-166, 2007.